International Journal of Research in Advance Engineering, (IJRAE)
Vol. 2, Issue 5, Sep-Oct-2016, Available at: **www.knowledgecuddle.com/index.php/IJRAE**

Development of cathode materials for magnesium primary cell

K. Narthana[1], M. Selvam[1], K. Saminathan, V. Rajendran and Karan V.I.S. Kaler[2]

[a]Centre for nano science and technology, K S Rangasamy College of technology,
Tiruchengode -637 215, Tamil Nadu, India

[b]Schulich School of Engineering , Department of Electrical and Computer Engineering, University of Calgary, Calgary, Alberta, Canada.

***Abstract*: The Zinc Sulfide nanoparticles were synthesized by simple chemical reaction of $ZnCl_2$ and Sulphur powder in aqueous solution. The main advantage of this method is the use of non-toxic precursors and water as solvent. The BZ1 and NZ2 samples reveal an average particle size respectively 510 and 43.7 nm. The structural, morphological, chemical composition and optical properties of the nanoparticles were investigated by X-ray diffraction, Scanning electron Microscopy, and Energy-dispersive X-ray Spectroscopy, Ultra Violet Spectroscopy and Electrochemical studies. The NZ2 sample showed a high discharge capacity of 362 mAh g^{-1}, whereas the BZ1 sample showed a discharge capacity of 120 mAh g^{-1}. The discharge capacity of NZ2 sample based cathode was 33.1 % higher than BZ1 sample based cathode. Thus, the above studies confirm that zinc sulfide nano powders show promise application as a cathode material for Mg/ZnS primary cell.**

Key words: BZ1 sample, NZ2 sample, Discharge capacity, Electro chemical studies, Band gap
*Corresponding author: selvamic@gmail.com

I. INTRODUCTION

In recent years, the increasing demand for high performance primary batteries with high energy density and low to moderate discharge capacity, employed in all portable and electronic devices, has stimulated research in the development and application of different types anode materials such as Mg, Zn, Na and Li [1]. Mg based anode materials are cost, safe, environmental friendly and offer high capacity however they are prone to a decrease in the charge and discharge cycling for energy consumption [2, 3]. More recently, the use of graphene or graphene based composites as an alternative electrode material has gained greater acceptance due to its high mechanical strength to volume ratio, large surface area and excellent electrical conductivity [4-8]. As a result, various research groups have explored the development of composite materials consisting of graphene and metal sulphides like ZnS, CdS and SnS [9-12].

Generally, crystalline ZnS is an important II-IV compound semiconductor with a wide direct energy band gap (3.7 eV), which has been successfully used in UV light emitting diodes, injection laser displays, efficient phosphors in flat-panel, photo catalysis, fuel cells, LED, non-linear optical and energy storage devices [13-19].

In order to leverage ZnS as an electrode material for primary battery applications with increase discharge capacity we need to develop suitable cathode electrodes using ZnS nanoparticles. ZnS nanoparticles may be synthesized using a variety of methods, such as chemical [20, 21], solvothermal route [22, 23], single-source molecular precursor [24, 25] and direct elemental reaction route [26, 27]. In order to avoid the agglomeration of ZnS nanoparticles, materials such as microgel, synthetic polymer, mesoporous silicate materials and other organic surfactants (sodium bis (2-ethyl hexyl) sulfosuccinate) are used as a supporting or stabilising material [28-30].

ZnS core/shell nanocrystals are used as an anode for photo catalyst in direct methanol fuel cells to increase the efficiency [31]. The ZnS synthesized employing hydrothermal method exhibits non-linear optical properties and find

eISSN: 2395-1648

INDEX COPERNICUS INTERNATIONAL

ICV 2014: 53.07 Standardized Value: 5.71

applications as an optical materials and photonic crystals [10]. The anodic material ZnS in lithium ion batteries shows higher efficiency than other type of anode materials due to its high defective surface area. The storage capacity of lithium ion based batteries with ZnS cathode has been reported to be high as 400 $mAhg^{-1}$ [31], however, there is limited data on the utility of ZnS in primary batteries. ZnS material at the nanoscale namely nanocrystals, nanowires and nanobelts show an excellent optoelectronic and optical performances, which are different from their bulk material values [32].

In the present study, bulk and nanoscale ZnS is used as a cathodic material for Mg/ZnS based primary cells in order to achieve a higher specific storage capacity. ZnS nanoparticles used in the development of the cathode were synthesized using a standard chemical process. The electrochemical performances of the ZnS cathode primary batteries was experimentally determined and based on discharge characteristics.

II. Materials and methods

2.1. Synthesis of Nano ZnS

All chemical reagents were purchased from Sigma Aldrich and were used without any further purification. The ZnS nanoparticles were synthesized by a chemical method. Initially, solutions of 0.1 M zinc chloride (1.362 g) and 0.1 M sulphur (3.2 g) were each prepared in 100 ml of demonized water. The prepared sulphur solution was added drop wise into the zinc chloride solution. The sample was stirred for 10 min using a magnetic stirrer. After 10 mins, the 5 M NaOH solution was added drop wise to obtain a pH value between 7 and 8. The solution at this point turned milky white which confirming the formation of ZnS nanoparticles suspension. The ZnS nanoparticles were harvested by centrifuging the colloidal suspension at 10,000 rpm for 30 min. The obtained residue was washed in ethanol/water solution several times to remove any unwanted impurities. The resulting ZnS nanoparticles sample in powder form was dried at 80^0 C for 2 h which was followed by another drying step in a hot air oven at 120 K for 2 h. The obtained ZnS nanoparticles are referred to as NZ2. Similarly, the bulk ZnS sample is referred to as BZ1.

2.2. Construction of Mg/ ZnS primary cell

Mg/ZnSprimary cell, used in the present study, was constructed to facilitate electrochemical measurements. Here, a circular shaped Mg pellet (13 mm in diameter and 3 mm thick) served as the anode material and was formed by pressing 0.5 g of Mg using a hydraulic pellet operated under at a pressure of 80 kg cm^{-3}. Similarly, a pellet comprised of activated carbon, ZnS nanoparticles and poly vinylidene difluoride (PVDF) at a weight ratio of (10:85:5), which served as the cathode, was formed using a hydraulic press operated at a pressure of 70 kg cm^{-3} of the same dimensions as the Mg pellet. The two pellets were housed in an insulating tube and separated from each other by Kraft sheet separator, which had previously been impregnated with a few drops of 0.1 M $MgCl_2$ (3 ml) electrolyte. Electrical contact to the anode and cathode pellets was achieved using two stainless steel (SS316L) semi-ball fitted with copper cylindrical plates. A schematic diagram of the primary cell used in this investigation is shown in Fig.1. A similar procedure was employed in the construction of the primary cell using commercially available (Sigma Aldrich) ZnS powder.

III. Characterisation

The X-ray diffraction study was used to determine the crystallographic structure of the prepared samples by recording the XRD pattern employing X-ray diffractrometer (X' pert Pro, Analytical, and The Netherland). The CuKα was used as the radiation source (1.5434 λ) with a constant voltage (40 kV) and current rating (30 mA) in the scan range of $10\text{-}80^0$ with an increment of 0.05^0 to obtain the XRD pattern of the compressed pellet samples.

eISSN: 2395-1648

INDEX COPERNICUS INTERNATIONAL

ICV 2014: 53.07 Standardized Value: 5.71

The morphology of samples was analyzed using a scanning electron microscope (SEM) (JEOL, JSM 5300 and Japan) and the microstructure features and composition of samples was determined employing an energy dispersive X-ray analysis (EDAX) (JEOL, JSM 5300 and Japan).

The absorption spectra of the prepared samples were determined employing UV-Visible spectrometer (Perkin Elmer Spectrophotometer, USA). Here, the samples were dispersed in solution at different dilutions. The prepare solutions were loaded in the square quartz cuvette and the spectral analysis at room temperature in the range of 300 to 400 nm.

The electrochemical discharge measurement was carried out employing Metrohm Auto lab (PGSTAT 302N, The Netherlands). The electrical discharge measurement of the constructed primary cells both with nano and bulk particles were carried out using galvanostatic constant discharge current of 5 mA with a cut off voltage of 0.2 V. Finally, the impedance measurements were carried using Metrohm Auto lab impedance analyzer over the frequency range of 1 mHz to 100 kHz at room temperature (303 K).

IV. Result and discussion

The X ray diffraction pattern of the samples BZ1 and NZ2 are shown in Fig.2. Samples BZ1 and NZ2 observed peaks corresponding to (111), (220), (311) and (331) planes which are related to existence of a cubic ZnS phase. However, the sample NZ2 shows additional peaks at (200) planes, which are associated with the illuminating the characteristic of Nano ZnS particles [19]. Thus, the obtained crystalline phase matched with standard diffraction pattern (JCPDS. No. 05-0566). In addition, the intensity of the sample BZ1 is lower than that of the sample NZ2, which is may be due to the presence of ZnS Nano crystalline structure. The average crystallite size of the samples BZ1 and NZ2 was calculated using the Scherer's formula. The obtained crystallite size of sample BZ1 and NZ2 are respectively 510 and 43.7 nm.

The UV absorption spectra of samples BZ1 and NZ2 are shown in Fig.3. The sample BZ1 and NZ2 exhibited an absorption edge at 350 and 320 nm respectively, which is active under the UV region. However, the absorption spectra of sample NZ2 extended further into the UV spectral range, compared to sample BZ1. The enhanced UV absorption for sample NZ2 is due to the size dependent properties of ZnS. The energy band gap of sample BZ1 and NZ2 is calculated using the energy equation.

$$E=hc/\lambda \qquad (i)$$

where h is the Planck's constant, c is the velocity of light and λ the wavelength.

The obtained band gap energy for the samples BZ1 and NZ2 is 3.8 and 3.5 eV respectively. The lower band gap energy of sample NZ2 used for electrochemical application, while it is belong to high storage capacity.

The SEM image of the samples BZ1 and NZ2 are shown in Fig.4. The surface morphology of the sample BZ1 reveals a rock shaped morphology with strong agglomeration of nanoparticles. On other hand, the surface morphology of NZ2 sample showed the presence of spherical shape particle with low level of agglomeration. The chemical composition analysis of samples BZ1 and NZ2 showed the presence of Zn, S, O and Cl without any impurities (insert table in Fig.4).

The primary cell electrode impedance was experimentally determined over a wide frequency range as shown in Fig.5. For a single electrode and the capacitor, a semicircle is obtained at high frequency in the range of 100 kHz to 10 Hz and a straight line at the low frequency region. The capacitor value is increased at low frequencies due to a larger number of moving ions which causes a decrease in the bulk resistance of the capacitor. On the other hand, in sample NZ2 the semicircle results from the parallel combination of resistance, capacitance while the obtained linear region is may be due to Warburg impedance. In the low frequency region, the linear region leans more towards imaginary axis and this indicates good capacitive behavior. The bode plots shows the frequency peak shift in NZ2 based 0.1 M Na_2SO_4 from 5.82 to 123 Hz. Bode plot also proves the increase in resistance by decrease in frequency, which results reduced self-discharge rate of ZnS Cathode.

The constructed Mg/ZnS primary cell was analyzed using galvanic constant current (5 mA) measurements. Fig.6. shows the characteristic discharge behavior of both the Mg/ZnS cell made from the bulk (sample BZ1) and Nano ZnS particles (sample NZ2). It is readily evident from Fig.6. NZ2 cell performed substantially better than BZ1 cell since its discharge rate is substainly slower than that of BZ1 and furthermore reaching a discharge plateau voltage of 0.8 V compared

eISSN: 2395-1648

INDEX COPERNICUS INTERNATIONAL

ICV 2014: 53.07 Standardized Value: 5.71

to 0.4 V for BZ1. Furthermore, sample NZ2 exhibited linear discharge characteristics during the discharge time 78,120 s (21.7 h) after which it exhibited a sharp drop in voltage at cutoff voltage of 0.4 V. In contrast sample BZ1 discharge process was much more rapid and attaining a discharge voltage plateau, within a short period of time (25,920 s (7.2 h)) with a cutoff voltage of 0.2 V. The discharge behavior of BZ1 is attributed to and influenced by electrode polarization electrodes. From fig.6. the observed flat line indicates that decaying voltage after the initial stage is mainly assigned to the high potential capacity of the sample NZ2 than sample NZ1. Moreover, the discharge capacity of the fabricated cell is calculated using the following equation,

$$Q = IT/m \qquad \text{(ii)}$$

Where I is the discharge current (5 mA), T is the discharge time until the cutoff voltage in seconds, and mass m in gms of the active material (cathode).

Based on equation (ii) and the discharge characteristics shown in Fig.6, Sample BZ1 has a discharge capacity of 120 $mAhg^{-1}$ while the sample NZ2 has a discharge capacity of 362 $mAhg^{-1}$.

V. CONCLUSION

In summary, we have chemically synthesized ZnS nanoparticles with high surface area to volume ratio and constructed an active cathode by mixing with conductive additives based on $MgCl_2$ (0.1 M) electrolytes used in an Mg/ZnS primary cell. For comparison purposes we also constructed a similar primary cell using commercial bulk material ZnS. The discharge performance of both these evaluated based on the discharge behavior. Among the two cathodes tested, the primary cell constructed using ZnS nanoparticles sample exhibited superior performance (discharge time =21 h) at a discharge current of 5 mA. The above finding suggests that an NZ2 based cathode is a promising alternative for Mg/ZnS primary batteries used in high power applications.

REFERENCES

[1] Peng B, Liang J, Tao Z, Chen J. Magnesium nanostructures for energy storage and conversion. Journal of Material Chemistry, 2009; 19, 2877.

[2] Srither S. R, Selvam M, Arunmetha S, Yuvakkumar R, Saminathan K, Rajendran V. Enhancement of Discharge Capacity of Mg/MnO_2 Primary Cell with Nano-MnO_2 as Cathode . Science and Advanced Materials, 2013; 5, 1–5**.**

[3] Calizo I, Balandin A. A, Bao W, Miao F, Lau C. N. Temperature Dependence of the Raman Spectra of Graphene and Graphene. Nano Letters, 2007; 7, 2645–2649

[4] Balandin A. A. Thermal properties of graphene and nanostructure carbon materials. Natural Materials, 2011; 10, 569-581.

[5] Nika D. L, Balandin A. A. Two-dimensional phonon transport in graphene. Journal of Physical Condensed Matter, 2012; 24, 233203.

[6] Ma Y, Zheng Y, Chen J.P. A zirconium nanoparticle for significantly enhanced sorption of arsenate: synthesis, characterization, measurement of performances, and mechanism study. Journal of Colloidal Interface Science, 2011; 354,785–792.

eISSN: 2395-1648

INDEX COPERNICUS INTERNATIONAL

ICV 2014: 53.07 Standardized Value: 5.71

[7] Srither S.R, Karthik A, Selvam M, Saminathan K, Rajendran V Karan V.I.S. Kaler. Nano sized MnO_2 particles produced by spray pyrolysis for a Zn/MnO_2 primary cell: comparative discharge performance studies with their bulk counterparts. RSC Advances, 2014; DOI: 10.1039/c4ra05060f

[8] Selvam M, Sakthipandi K, Suryaprabha R, Saminathan K, Rajendran V**.** Synthesis and characterization of electrochemically – reduced graphene. Bulletin of Material Sciences, 2013; 36 (7), 1315-21.

[9] Shen, Chenfei Zheng, Mingbo Xue, Luping Li, Nianwu Lü, Hongling Zhang, Songtao Cao, Jieming, Chin. Preparation of Graphene-ZnS Nanocomposites via Hydrothermal Method Using Two Sulfide Sources. Journal of Chemistry, 2012; 29, 719-723.

[10] Meyer J. C, Geim A. K, Katsnelson M. I, Novoselov K. S, Booth T. J, and Roth S. The structure of suspended graphene sheets. Nature, 2007; 446, 60–63.

[11] Xu C, Xu B, Gu Y, Xiong Z, Sunb J, Zhao X. S. Graphene-based electrodes for electrochemical energy storage. Energy Environmental Science, 2013; 6, 1388-1414.

[12] John R, Sasi Florence S. Optical, Structural And Morphological Studies Of Bean- Like Zns Nanostructures By Aqueous Chemical Method. Chalcogenide Letters, 2010; 7(4), 269-273.

[13] Pan S, Liu X. ZnS–Graphene nanocomposite: Synthesis, characterization and optical properties. Journal of Solid State Chemistry, 2012; 191, 51-56.

[14] Simya O.K, Selvam M, Karthik A, Rajendran V. Dye-sensitized solar cells based on visible-light-active TiO_2 heterojunction nanoparticles. Synthetic Metals, 2014; 188:124– 129.

[15] Chen-Ho Lai, Ming-Yen Lu, Lih-Juann Chen. Metal sulfide nanostructures: synthesis, properties and applications in energy conversion and storage. Journal of Material Chemistry, 2012; 22, 19-30**.**

[16] Uekawa N, Matsumoto T, Kojima T, Shiba F, Kakegawa K. Synthesis of stable sol of ZnS nanoparticles by heating the mixture of ZnS precipitate and ethylene glycol. Colloids and Surfaces A: Physicochemical Engineering, 2010; 361,132–137.

[17] Saravanan N, Geok Bee Teh, Samuel Yong Peen Yap, Kar Mun Cheong. Simple synthesis of ZnS nanoparticles in alkaline medium. Journal of Materials Science: Materials in Electronics, 2008; 19, 1206–1208.

[18] Xu J, Ji. W. Characterization of ZnS nanoparticles prepared by new route. Journal of Materials Science Letters, 1999; 18, 115-117.

[19] Ibanga E.J, Le Luyer C, Mugnier J. Zinc oxide waveguide produced by thermal oxidation of chemical bath deposited zinc sulphide thin films Matter. Chemical Physics, 2003; 80, 490.

[20] Archana J, Navaneethan M, Ponnuswamy S, Hayakawa Y, Muthamizhchelvan C. Optical, structural and surface morphological studies of bean-like triethylamine capped zinc selenide nanostructures. Material Letters, 2009; 63,1931.

[21] Charinpanitkul T, Chanagul A, Dutta J, Rungsardthong U, Tanthapanichakoon W. Effects of co surfactant on ZnS nanoparticle synthesis in micro emulsion. Science and Technology of Advanced Materials, 2005; 6, 266–271.

[22] Yu S.H, Yoshimura M**.** Shape and Phase Control of ZnS Nanocrystals: Template Fabrication of Wurtzite ZnS Single-Crystal Nanosheets and ZnO Flake-like Dendrites from a Lamellar Molecular Precursor ZnS (NH2CH2CH2NH2)0.5. Advanced Materials, 2002; 14, 296–300.

[23] Liu W. Low temperature synthesis of hexagonal phase ZnS nanocrystals by thermolysis of an air-stable single-source molecular precursor in air. Material Letters, 2006; 60, 551–554.

[24] Malik M.A, Revaprasadu N. Air-stable single-source precursors for the synthesis of chalcogenide semiconductor nanoparticles. Chemistry of Materials, 2001; 13, 913–920.

[25] Li Y.D, Ding Y, Zhang Y, Qian Y.T. Photo physical properties of ZnS quantum dots. Journal of Physics and Chemistry of Solids, 1999; 60, 13–15.

[26] Verma A.K, Rauchfuss T.B, Wilson S.R. Solvent Mediated Reactions Of Elemental Zinc and Sulfur, Sans Explosion. Inorganic Chemistry, 1995; 34, 3072–3078.

[27] Pich A, Hain J, Lu Y, Boyko V, Prots Y. Hybrid Microgels with ZnS Inclusions. Macromolecules, 2005; 38, 6610–6619.

[28] Turner E.A, Huang Y.N, Corrigan J.F, Synthetic Routes to the Encapsulation *of II*–VI Semiconductors *in* Mesoporous Hosts. European Journal of Inorganic Chemistry, 2005; 22 , 4465–4478.

[29] Zhang J, Xiao M, Liu Z, Han B, Jiang T, He J, Yang G. Preparation of ZnS/CdS composite nanoparticles by co precipitation from reverse micelles using CO_2 as antisolvent. Journal of Colloid and Interface Science, 2004; 273, 160–164.

[30] Wei-Ta Chen,Yin-Kai Lin,Ting-Ting Yang, Ying-Chih Pu, Yung-Jung Hsu. Au/ZnS core/shell nanocrystals as an efficient anode photocatalyst in direct methanol fuel cells**.** Chemical Communications, 2013; 49, 8486-8488.

[31] Wang J, Wang G, Li Yang See How Ng, Liu H. An investigation on electrochemical behavior of nanosize zinc sulfide electrode in lithium-ion cells. Journal of Solid State Electrochemistry, 2006; 10, 250–254.

[32] Behboudni M, Majlesar M.H, Khanbabae B. Preparation of ZnS nanorods by ultrasonic waves. Materials Science and Engineering: B, 2005; 122, 160.

Figure captions

Fig.1.Schematic diagram of primary cell set-up

Fig.2. XRD pattern of BZ1 and NZ2 samples

Fig.3. UV charactersation of BZ1 and NZ2 samples

eISSN: 2395-1648

INDEX COPERNICUS INTERNATIONAL

ICV 2014: 53.07 Standardized Value: 5.71

Fig.4. SEM and EDAX pattern of both BZ1 and NZ2 samples

Fig. 5. Electrochemical impedance curve for BZ1 and NZ2 in 0.1 M Na_2SO_4

Fig.6. Discharge potential as a function of time for both BZ1 and NZ2 samples

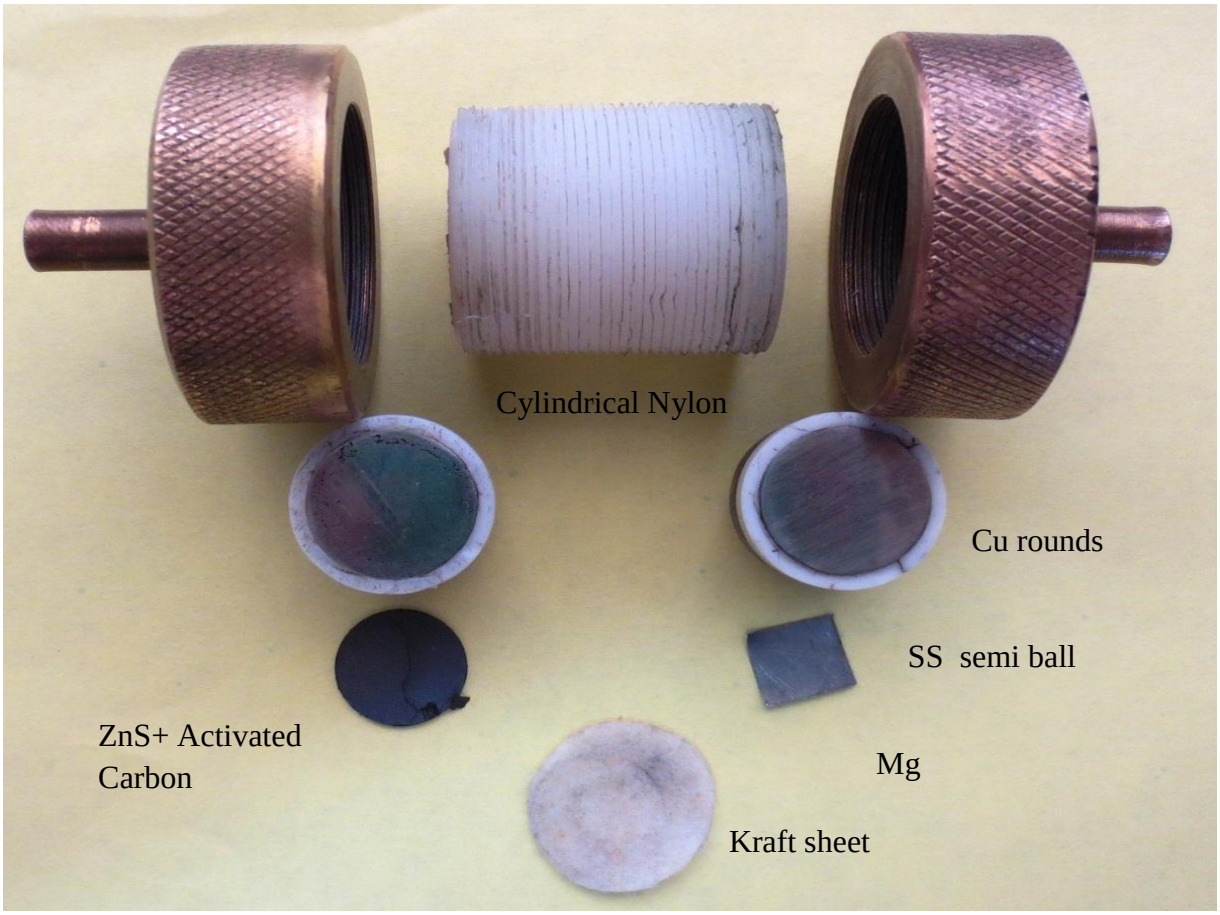

Fig. 1 Schematic diagram of primary cell setup

eISSN: 2395-1648

INDEX COPERNICUS INTERNATIONAL

ICV 2014: 53.07 Standardized Value: 5.71

eISSN: 2395-1648

ICV 2014: 53.07 Standardized Value: 5.71

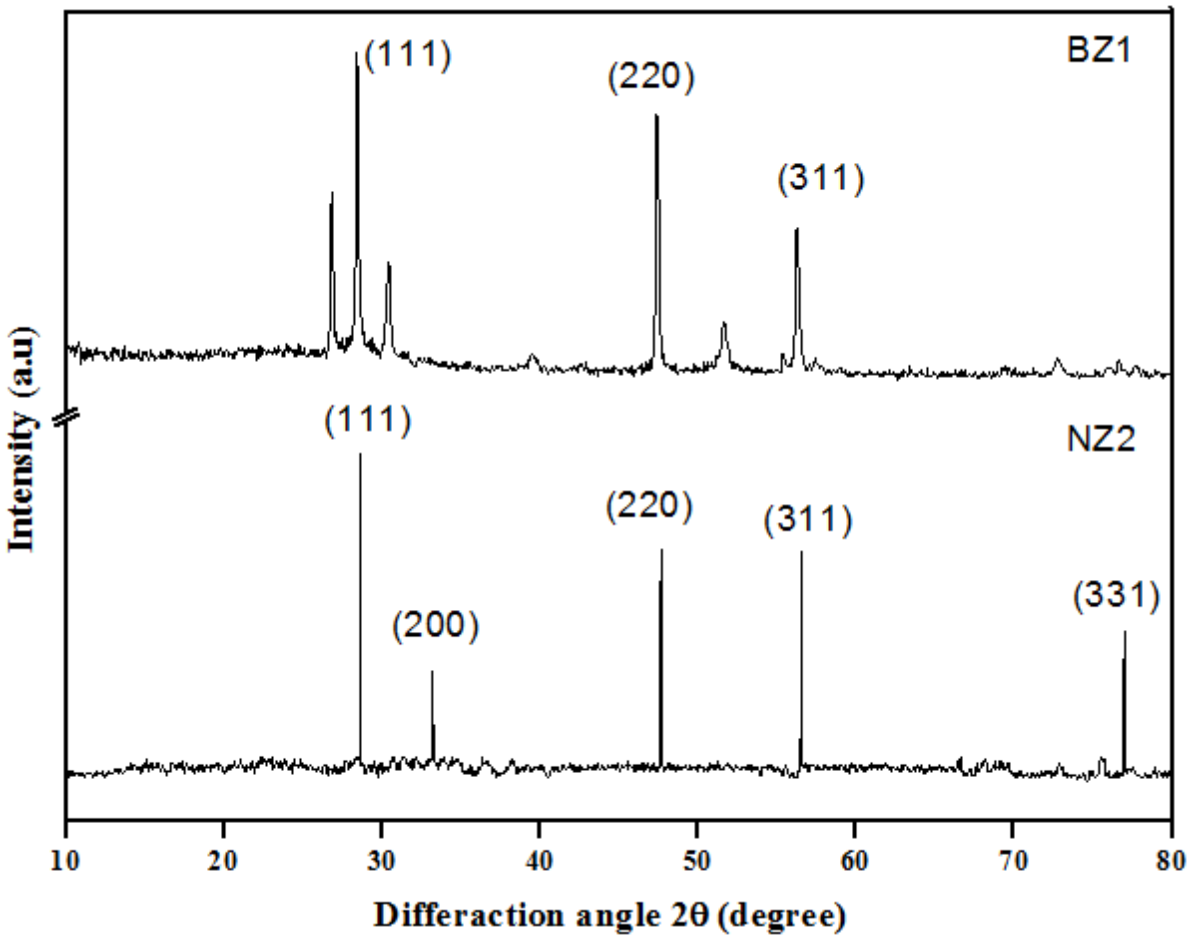

Fig.2. XRD pattern of BZ1 and NZ2 samples

eISSN: 2395-1648

INDEX COPERNICUS INTERNATIONAL

ICV 2014: 53.07 Standardized Value: 5.71

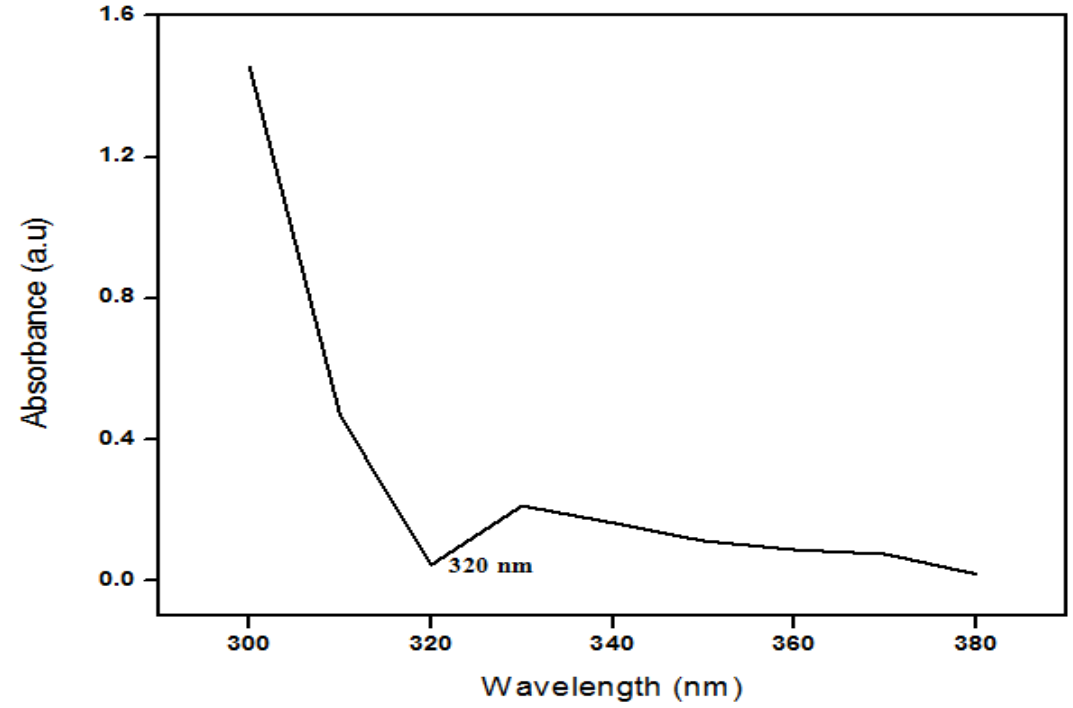

i) Sample BZ1

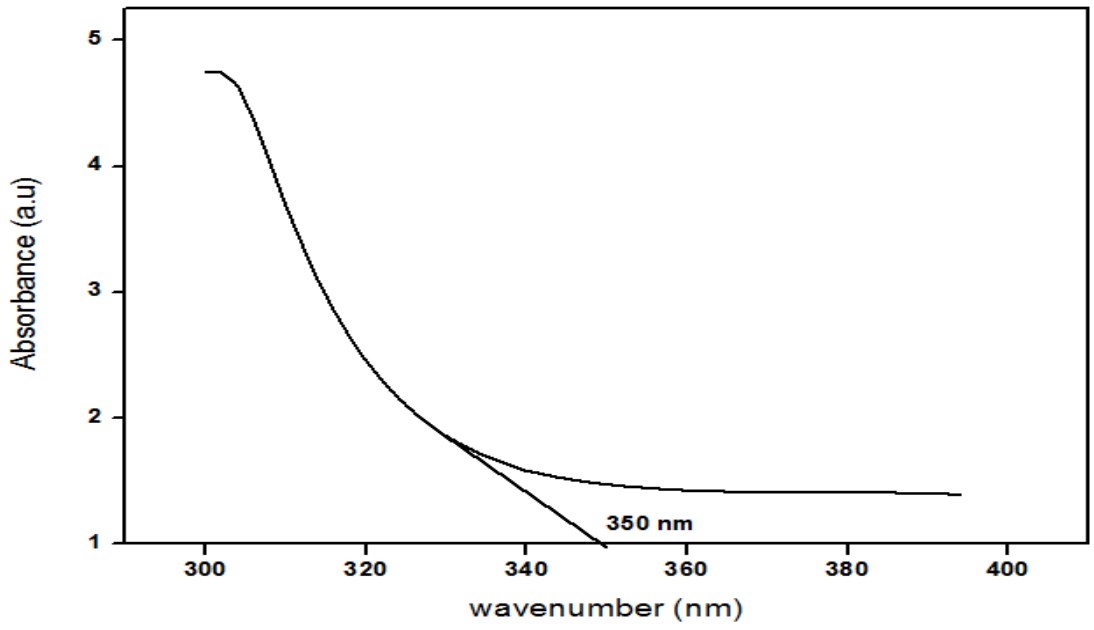

ii) Sample NZ2

Fig.3. UV charactersation of BZ1 and NZ2 samples

eISSN: 2395-1648

INDEX COPERNICUS INTERNATIONAL

ICV 2014: 53.07 Standardized Value: 5.71

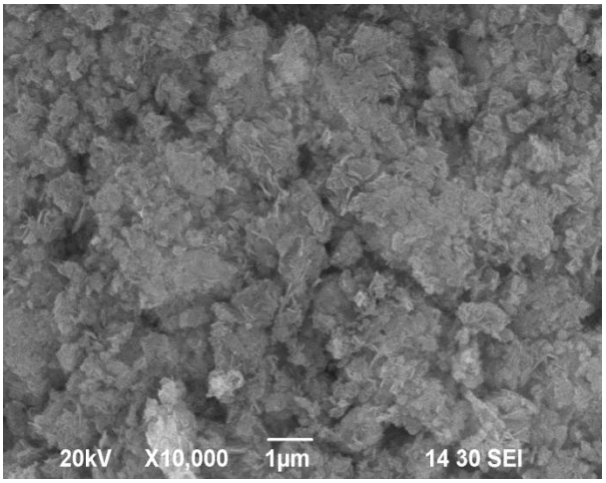

i) SEM image

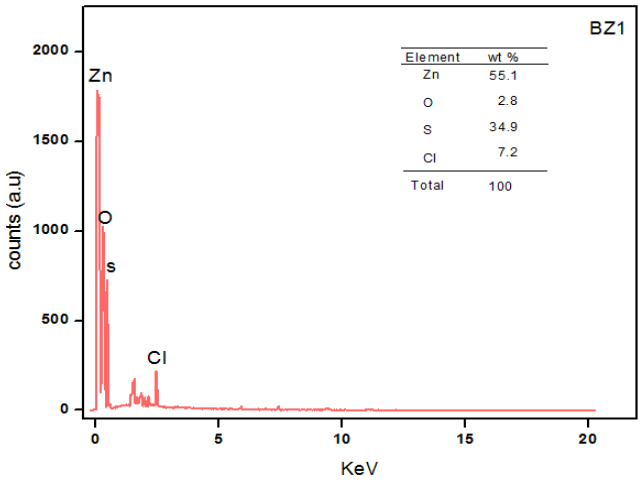

ii) EDAX pattern

a) Sample BZ1

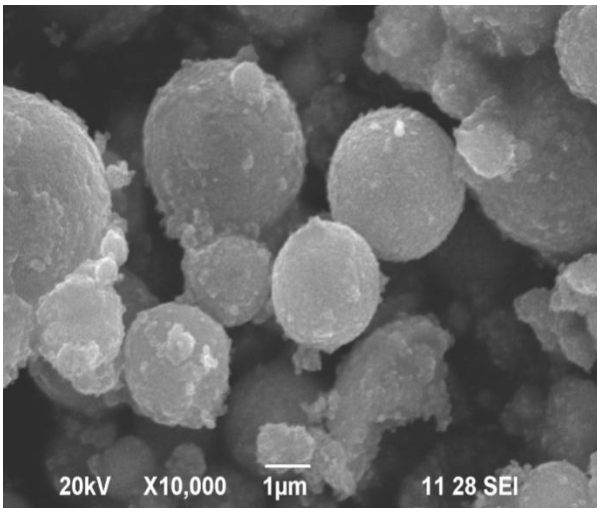

i) SEM image

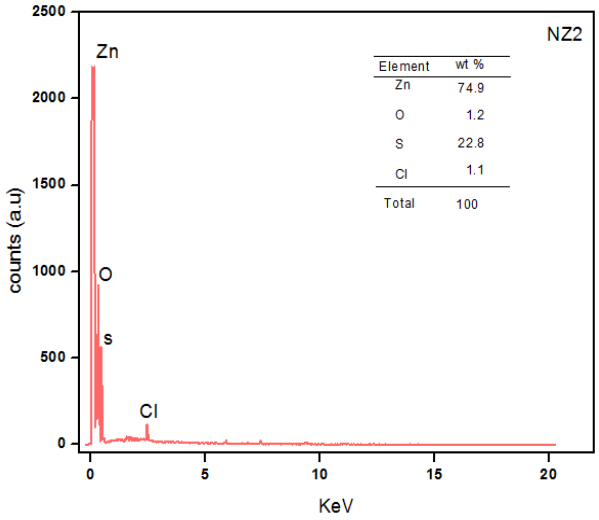

ii) EDAX pattern

b) Sample NZ2

Fig.4. SEM and EDAX pattern of both BZ1 and NZ2 samples

eISSN: 2395-1648

INDEX COPERNICUS INTERNATIONAL

ICV 2014: 53.07 Standardized Value: 5.71

i) Nyquist plot of BZ1

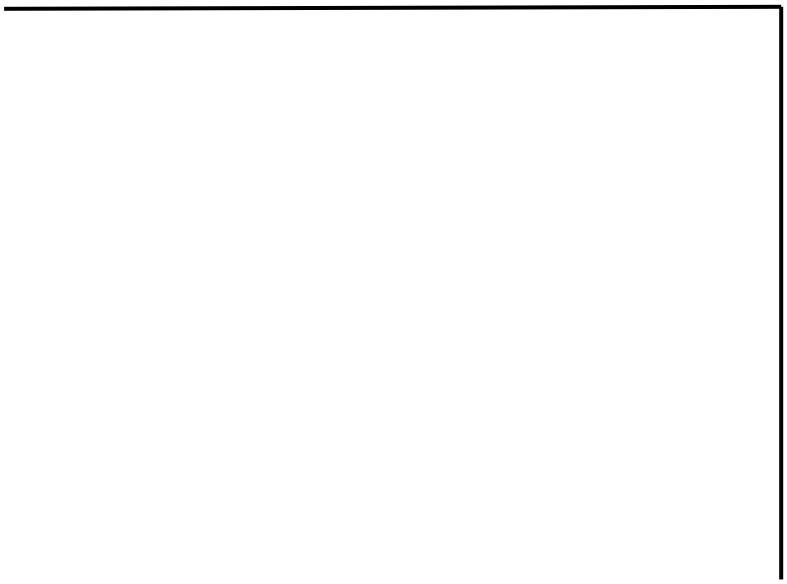

ii) Nyquist plot of NZ2

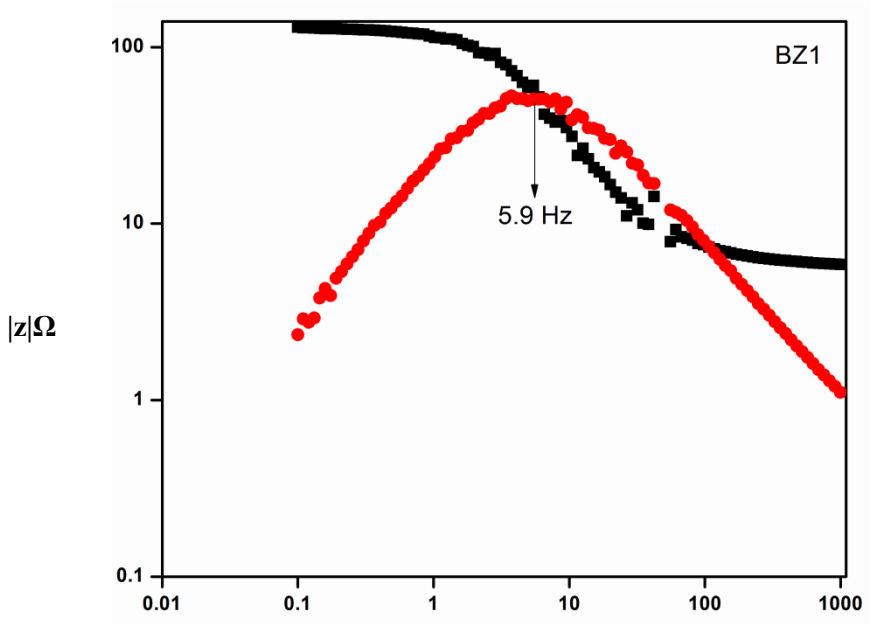

eISSN: 2395-1648

INDEX COPERNICUS INTERNATIONAL

ICV 2014: 53.07 Standardized Value: 5.71

iii) Bode plot for BZ1

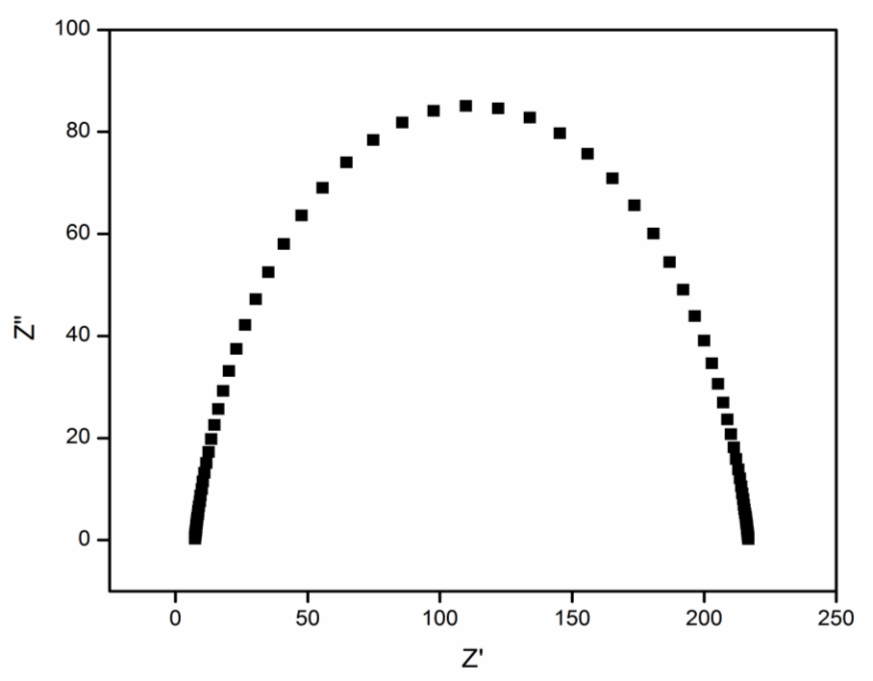

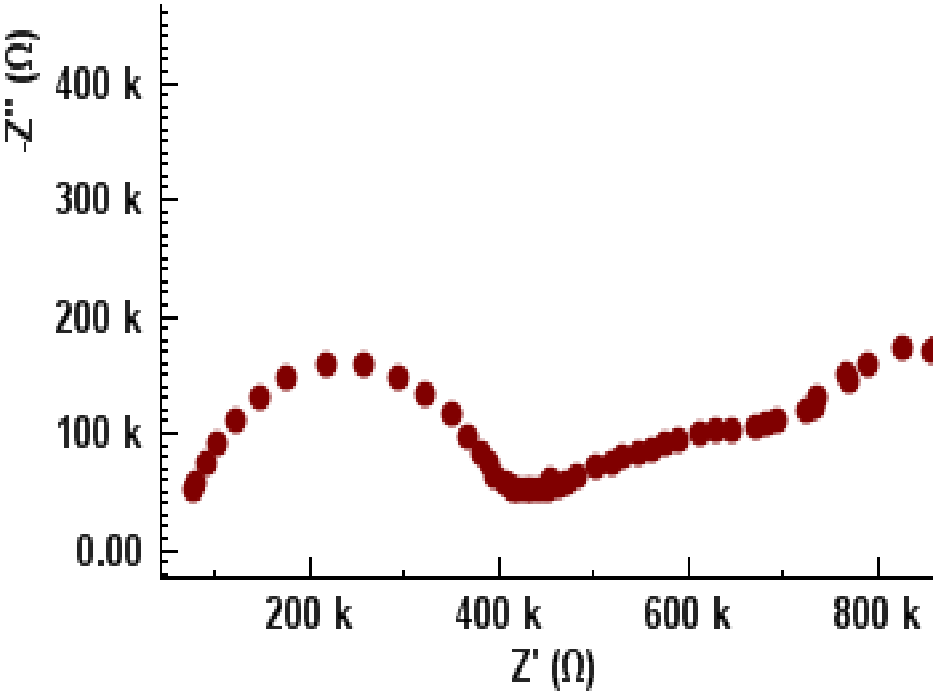

eISSN: 2395-1648

INDEX COPERNICUS INTERNATIONAL

ICV 2014: 53.07 Standardized Value: 5.71

iv) Bode plot for NZ2

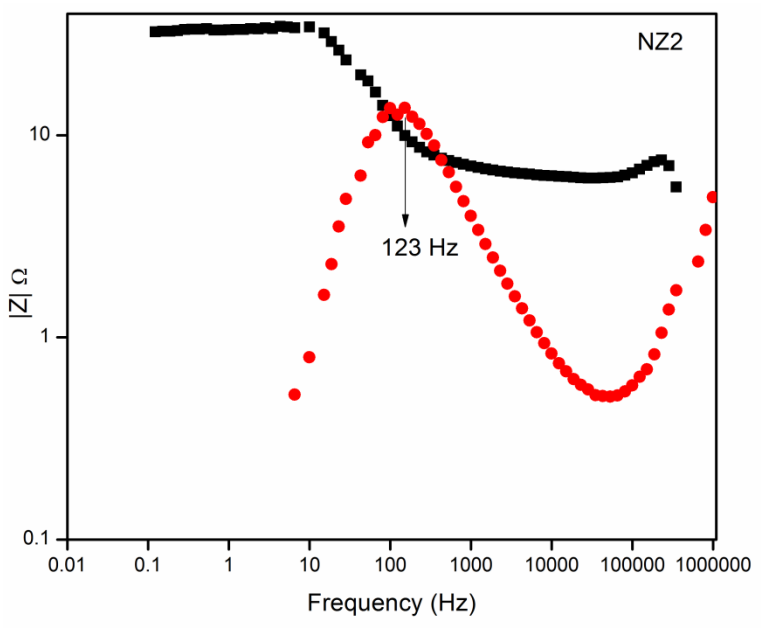

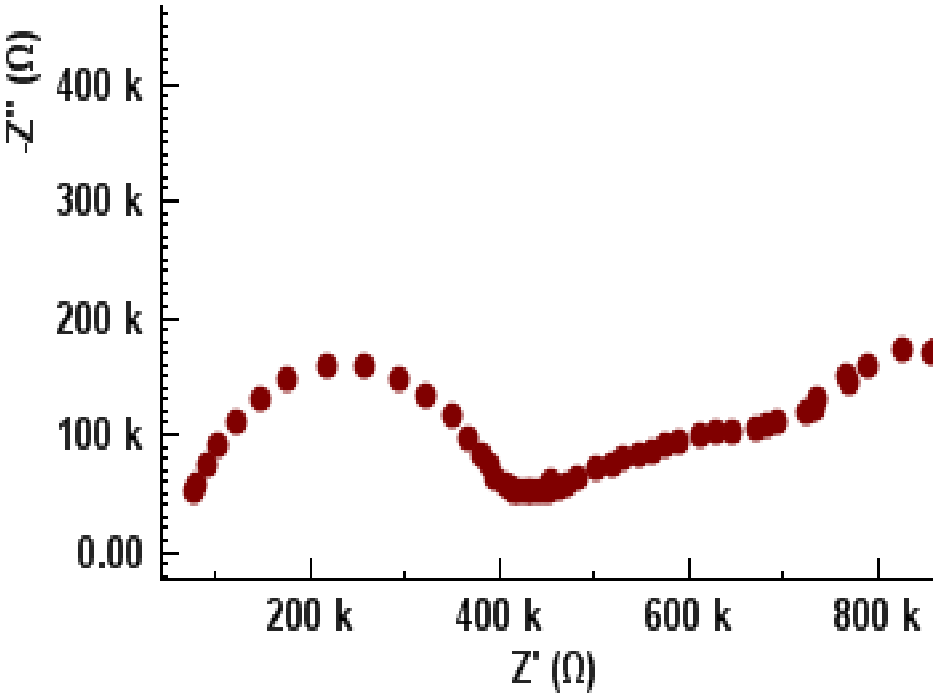

eISSN: 2395-1648

INDEX COPERNICUS INTERNATIONAL

ICV 2014: 53.07 Standardized Value: 5.71

Fig. 5. Electrochemical impedance curve for BZ1 and NZ2 in 0.1 M Na_2SO_4

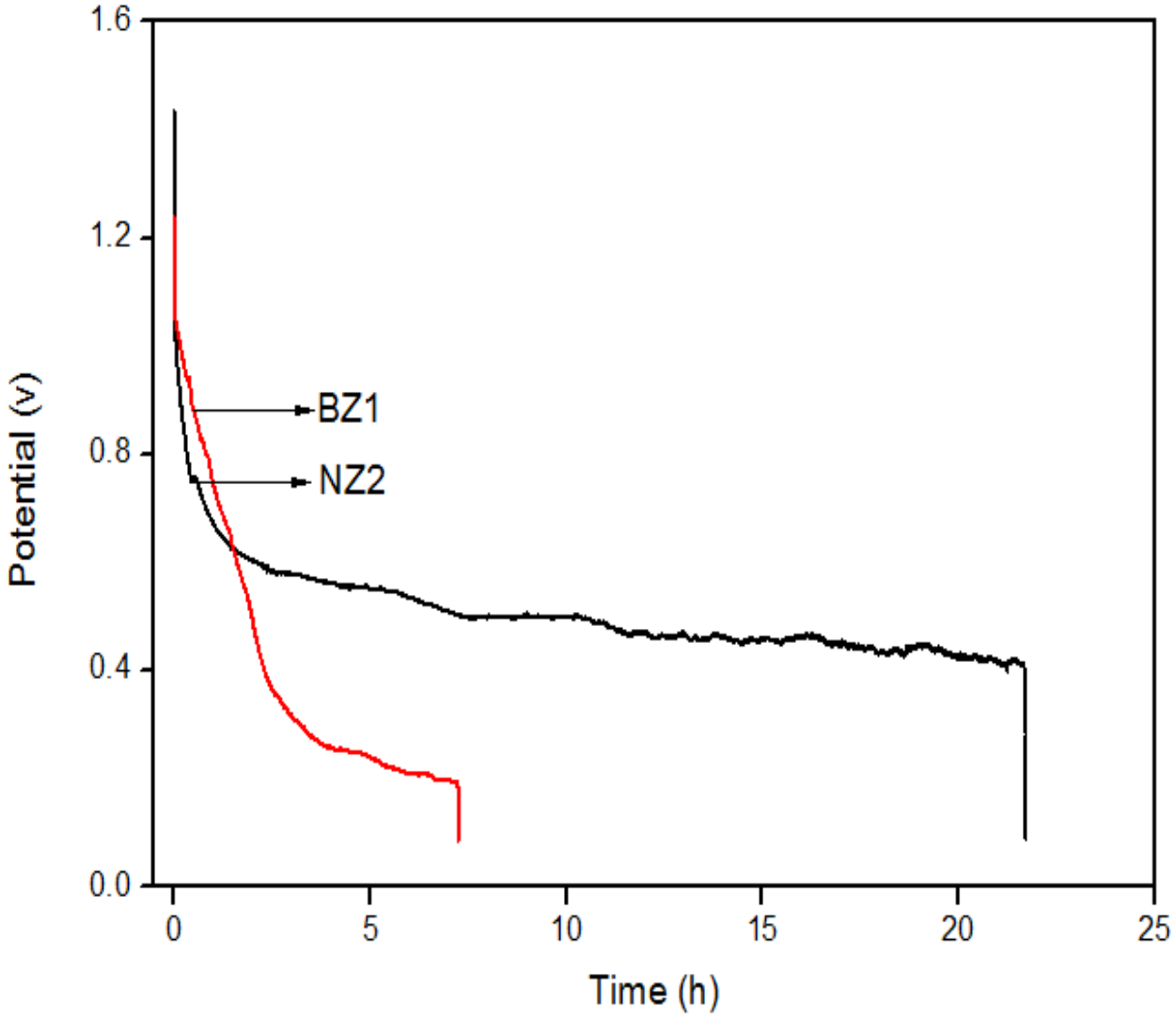

Fig.6. Discharge potential as a function of time for both BZ1 and NZ2 samples

eISSN: 2395-1648

INDEX COPERNICUS INTERNATIONAL

ICV 2014: 53.07 Standardized Value: 5.71